

Spectral and thermodynamic properties of a strong-leg quantum spin ladder

D. Schmidiger,¹ P. Bouillot,² S. Mühlbauer,¹ S. Gvasaliya,¹ C. Kollath,³ T. Giamarchi,² and A. Zheludev^{1,*}

¹*Neutron Scattering and Magnetism, Laboratory for Solid State Physics, ETH Zurich, Switzerland.*

²*DPMC-MaNEP, University of Geneva, CH-1211 Geneva, Switzerland.*

³*DPT-MaNEP, University of Geneva, CH-1211 Geneva, Switzerland.*

(Dated: November 11, 2018)

The strong-leg $S = 1/2$ Heisenberg spin ladder system $(\text{C}_7\text{H}_{10}\text{N})_2\text{CuBr}_4$ is investigated using Density Matrix Renormalization Group (DMRG) calculations, inelastic neutron scattering, and bulk magneto-thermodynamic measurements. Measurements showed qualitative differences compared to the strong-rung case. A long-lived two-triplon bound state is confirmed to persist across most of the Brillouin zone in zero field. In applied fields, in the Tomonaga-Luttinger spin liquid phase, elementary excitations are attractive, rather than repulsive. In the presence of weak inter-ladder interactions, the strong-leg system is considerably more prone to 3-dimensional ordering.

In quantum magnets, the interplay between exchange and quantum fluctuations leads to a host of novel phases, much richer than their classical counterparts. In particular, correlations between the spins can be strongly suppressed by quantum effects, leading to quantum *spin liquid* phases with properties quite different from those of any conventional ferro- or antiferromagnet. Under magnetic fields these systems undergo quantum phase transitions that are akin to Bose-Einstein condensation [1]. Among the spin liquids, antiferromagnetic (AF) Heisenberg $S = 1/2$ ladders are the simplest, yet perhaps the most important and extensively studied [2]. They combine the essence of quantum magnetism with peculiar features that stem from their one dimensional nature [3]. As a result, in applied fields they demonstrate a variety of scaling properties, characteristic of the physics of one dimensional interacting quantum particles, the so called Tomonaga Luttinger liquids (TLL). Understanding which key parameters of the actual spin Hamiltonian control these universal features is a formidable challenge that requires novel experimental and theoretical approaches.

In recent years, a general theory of weakly coupled ladders under strong magnetic fields has emerged [4]. Considerable experimental progress in understanding *strong-rung* spin ladders was made through the study of the compounds IPA-CuCl₃ [5–7] and BPCB [8–13]. Particular attention was given to the field-induced quantum phase transitions [6–8, 10, 11], and the properties of the gapless TLL critical phase at intermediate fields [10, 12].

In the case of the strong rung ladder, the spin gap in the absence of a magnetic field is already present on each rung, protecting the spin-liquid state from the leg exchange. A more subtle limit is provided by the strong leg (or weak rung) ladder. In that case the existence of a spin liquid state is far from obvious, and results [2] from an Haldane gap mechanism [14]. This leads to some similarities between the two limits but of course also to important differences, in terms of the origin of the spin gap, excitation spectrum, and the TLL mapping. On the experimental side, this interesting problem remained elusive since only few studies are available.

In this paper we report both experimental and theoretical studies of the prototypical strong-leg spin ladder material DIMPY [15, 16]. We determine both its thermodynamic properties and the neutron scattering spectrum, and show how to use these data to determine the TLL parameters in the strong-leg case. A remarkable quantitative agreement with DMRG calculations gives us a precise description of the material, needed to understand long range ordering detected at low temperatures.

The magnetic properties of DIMPY originate from ladders formed by $S = 1/2$ Cu²⁺ ions, that run along the a axis of the monoclinic crystal structure [18]. We model this compound by the AF Heisenberg two-leg spin ladder Hamiltonian

$$\mathcal{H} = J_{\text{leg}} \sum_{l,j} \mathbf{S}_{l,j} \cdot \mathbf{S}_{l+1,j} + J_{\text{rung}} \sum_l \mathbf{S}_{l,1} \cdot \mathbf{S}_{l,2} - g\mu_B H \sum_{l,j} S_{l,j}^z.$$

Here J_{leg} and J_{rung} are the couplings along the leg and rung, respectively, $g\mu_B H$ is the uniform Zeeman field, and $\mathbf{S}_{l,j}$ are the spin operators acting on site l of the leg j of the ladder. At $H = 0$, the ground state of DIMPY is a non-magnetic spin singlet separated from the lowest-energy triplet excited states by an energy gap of $\Delta = 0.36$ meV [15, 16]. Previous studies suggested that the application of a magnetic field at $T \rightarrow 0$ leads to a quantum phase transition to the TLL state at $H_{c1} = 2.85$ T [15]. Inelastic neutron scattering measurements of the dispersion relation for triplon excitations yielded an estimate of the ratio of exchange constants as $J_{\text{leg}}/J_{\text{rung}} \sim 2.2$, through a comparison with theoretical results obtained with the PCUT method [15]. A more detailed measurement over the whole Brillouin zone confirmed that the spin Hamiltonian is symmetric with respect to leg permutation [16]. This feature allows one to conveniently describe the spin dynamics in terms of separate *antisymmetric* (leg-odd “-”) and *symmetric* (leg-even “+”) structure factors

$$\mathcal{S}^{(\pm)}(q, \omega) \propto \sum_{\lambda} |\langle \lambda | \mathbf{S}_{\pm}(q) | 0 \rangle|^2 \delta(\omega + E_0 - E_{\lambda}),$$

respectively. Here $|0\rangle$ denotes the ground state of \mathcal{H} with

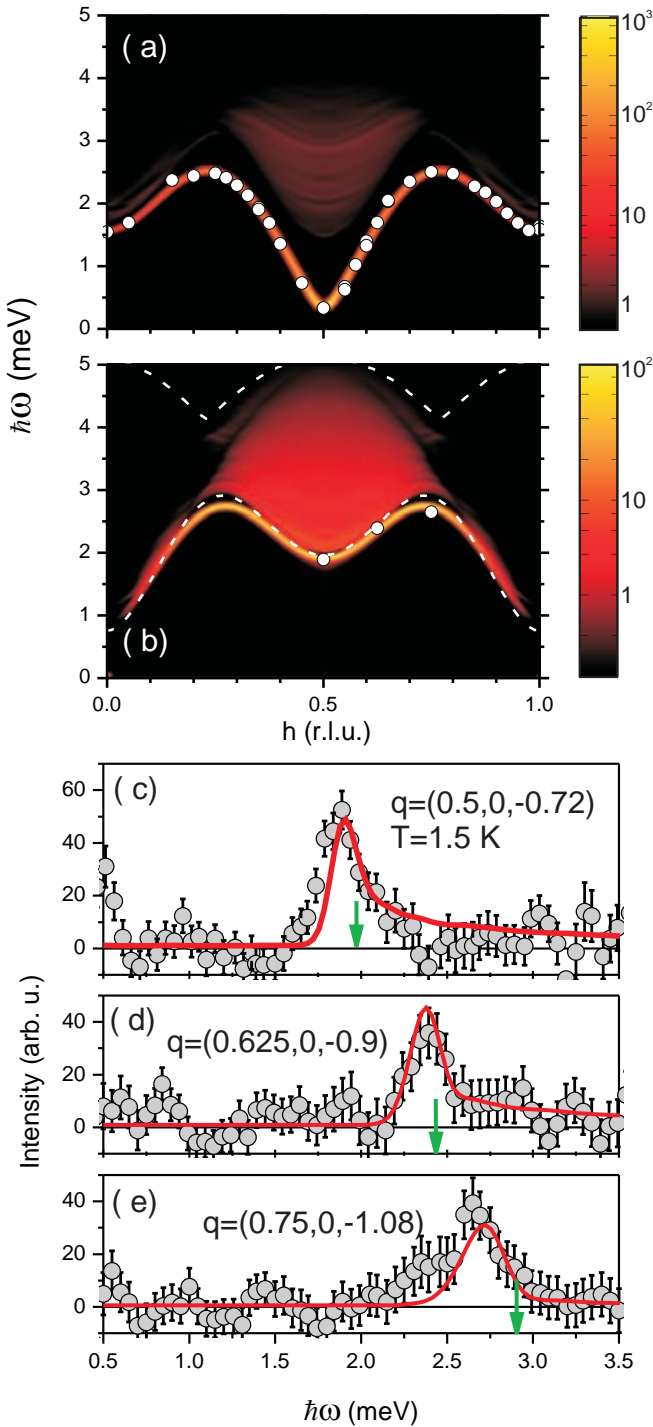


FIG. 1. (color online) Dynamic spin structure factor of DIMPY. (a) Antisymmetric channel. The false-color plot shows the DMRG result^a. Symbols are experimental data for single-triplon dispersion from Ref. [16]. (b) Symmetric channel. False-color plot as above. Symbols are positions of peaks in inelastic neutron scattering scans shown in (c)-(e) (symbols). The white dashed lines in (b) are the limits of the two triplons continuum. The solid red line in (c)-(e) is the DMRG result scaled by an arbitrary factor and convolved with the resolution function of the 3-axis spectrometer [17]. The green arrow in (c)-(e) is the lower edge of the two triplons continuum.

^a The oscillations are numerical artefacts.

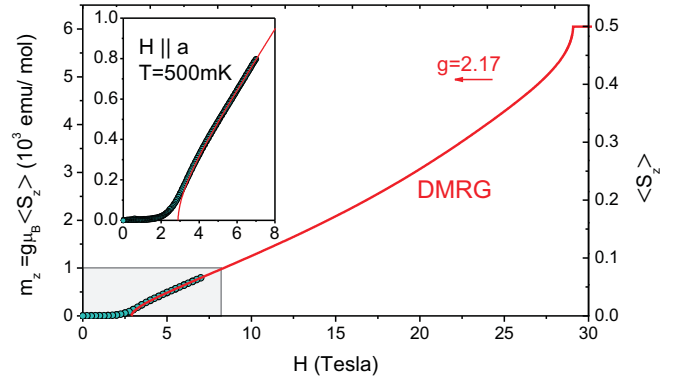


FIG. 2. (color online) Magnetization induced in DIMPY as a function of applied field. Symbols are the experimental data obtained for $H \parallel a$ at $T = 500$ mK. The solid line is a $T = 0$ DMRG calculation. The inset shows a blowup of the low-field region.

energy E_0 , $S_{\pm}(q) = \sum_l e^{-iq_l a} (S_{l,1} \pm S_{l,2})$, a the lattice constant, and \sum_{λ} is the sum over all eigenstates $|\lambda\rangle$ of \mathcal{H} with energy E_{λ} . The two channels can be independently probed by inelastic neutron scattering experiments.

To validate the spin Hamiltonian and to obtain a more accurate estimate of the $J_{\text{leg}}/J_{\text{rung}}$ ratio, we fit the experimental results of Ref. [16] for the *full* single-triplon dispersion present in $\mathcal{S}^{(-)}(q, \omega)$ with quasi-exact numerical results adjusting both J_{leg} and J_{rung} . The calculations were performed using the time-dependent DMRG method [19, 20] (for specific details see [21]). An almost perfect agreement with experiment is obtained over the whole Brillouin zone (BZ) with $J_{\text{leg}} = 1.42(6)$ meV and $J_{\text{rung}} = 0.82(2)$ meV shown in Fig. 1(a) [22]. The excellent agreement with data validates that \mathcal{H} is a faithful description of the system, and that additional terms (anisotropies, Dzialoshinski-Moryia etc.) if present are extremely small. We obtain $J_{\text{leg}}/J_{\text{rung}} = 1.72(6)$ for DIMPY, which is notably less than the value quoted in Ref. [15]. The main difference occurs in J_{leg} , and we attribute this difference to the approximation within the PCUT method [15] and to fitting in the whole BZ in our case.

The obtained exchange constants were used to calculate the symmetric structure factor $\mathcal{S}^{(+)}(q, \omega)$. In the strong-rung limit these excitations are attributed to multi-particle states with an even number of triplons [23, 24]. Assuming no interactions between excitations, one expects to see a diffuse continuum of two-triplon scattering with a *maximum* of the lower boundary at the center of the BZ $ka = \pi$. Interactions lead to two-triplon bound states [25]. In the strong rung limit, these only exist below the continuum in a narrow range close to the BZ-center. The actual calculated symmetric spectrum for DIMPY is shown in Fig. 1(b) and deviates from this simplistic picture. Similarly to the isotropic point ($J_{\text{leg}} = J_{\text{rung}}$) [26], the continuum has a local *minimum*

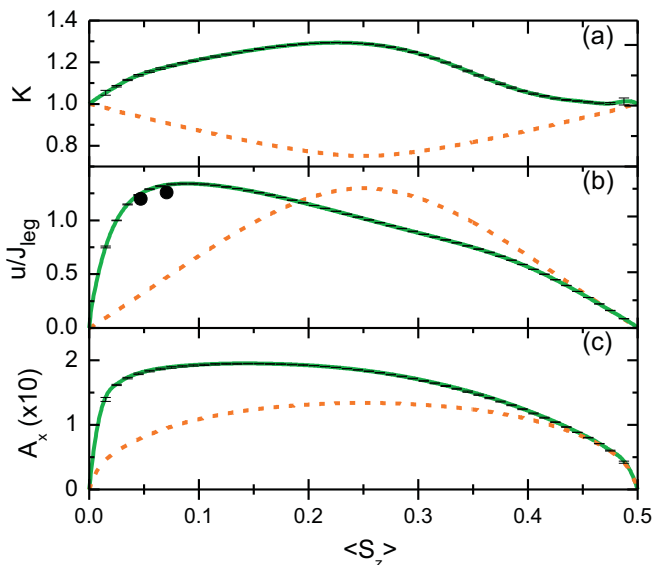


FIG. 3. (color online) TLL parameters as a function of field-induced magnetization. DMRG results determined following Ref. [21, 29] for DIMPY with $J_{\text{leg}}/J_{\text{rung}} = 1.72(6)$ are shown as solid lines and the strong-rung coupling limit as dashed lines [21]. The symbols in (b) are extracted from the experimental heat capacity measurement.

in the center of the BZ, where most of the spectral weight is concentrated. A characteristic 'hat' on top of the continuum can be identified. However, the most prominent feature is a long-lived excitation below the boundary of the continuum, stable across most of the BZ, at $0.8 \cdot 2\pi \gtrsim ka \gtrsim 0.2 \cdot 2\pi$. Numerically, integrating the singular and non-singular parts of the dynamic structure factor up to 5 meV, we estimate that 56% of the spectral weight is contained in single-triplon excitations and 14% in two-triplon bound states.

The theoretical results were tested in inelastic neutron experiments at the TASP 3-axis spectrometer at Paul Scherrer Institute, using the same deuterated single crystal samples and experimental conditions as in Ref. [16]. Typical constant- q scans measured at $T = 1.5$ K at several wave vectors that correspond to $\mathcal{S}^{(+)}(q, \omega)$ are shown in Fig. 1(c-e) in symbols [27]. The only adjustable parameter is an overall scale factor. The quantitative agreement between theory and experiment is a spectacular validation of our approach. In particular, it is possible to experimentally separate the bound state from the continuum. This is more delicate in strongly dimerized compounds [28], or those with large energy scales [24].

The fitted Hamiltonian also allows us to interpret bulk magnetometric experiments. The measured magnetization curve [30], for a field applied along the a axis at $T = 500$ mK is in excellent agreement with DMRG results as shown in Fig. 2. The small discrepancy in the very vicinity of H_{c1} being due to finite- T effects. The onset of magnetization signals the gapless TLL regime.

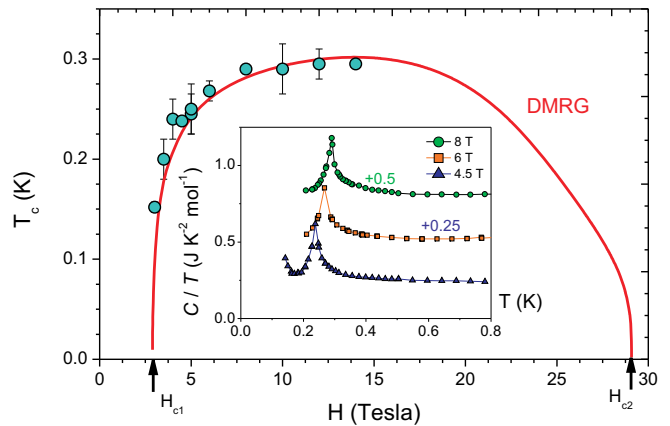


FIG. 4. (color online) Inset: Magnetic specific heat measured in DIMPY in fields applied along the b axis. Main panel: Field-temperature phase diagram of DIMPY. The area between H_{c1} and H_{c2} is the ordered state. Circles are positions of lambda-anomalies in specific heat. The solid line is the DMRG result using the adjustable parameter nJ_{MF} .

Here, the low-frequency long wavelength correlation functions and other properties are expected to have a universal form determined by the so-called Luttinger parameter K , which defines the powers of the algebraic correlations, and the velocity u of the linear excitation spectrum.

In DIMPY, these field dependencies are markedly different from those in the strong-coupling limit as shown in Figs. 3(a,b). In the latter case, K decreases beyond H_{c1} , and returns to unity at saturation H_{c2} . Throughout the TLL phase $K < 1$, and the elementary spin excitations (spinons) are *repulsive*. Not so in the strong-leg ladder. For DIMPY we see that K increases beyond H_{c1} and remains greater than unity at higher fields. This signifies an *attractive* interaction between spinons [4]. In the direct proximity of saturation at H_{c2} , $K \sim 1$, which corresponds to non-interacting spinons. The velocity u in DIMPY also behaves quite differently compared to the strong-rung coupling case, showing a strongly asymmetric behavior. This behavior of the velocity will have a strong influence on numerous quantities defined by low-energy excitations, such as the low energy continuum in the gapless phase. As a consistency check, we estimated the velocity additionally from the specific heat measurements discussed below, using the relation $C(T) = \frac{\pi k_B T}{6u}$, where C is normalized per spin [31]. This estimate (symbols in Fig. 3b) are in good agreement with our calculated velocity, in particular, considering that the determination by the specific heat can be inaccurate, as detailed in [21].

TLL physics is endemic to one dimension. Ironically, one of the most accurate ways to probe its properties is to study the *quasi*-1D case of weakly coupled ladders. Inter-ladder interactions result in three-dimensional long range AF ordering at a finite temperature. Assuming unfrustrated and weak couplings, the problem can be treated

in the framework of the chain-mean field (MF) theory [32]. The characteristics of the ordered state are entirely defined by the TLL properties of isolated ladders, with only one added parameter: the effective inter-ladder coupling constant nJ'_{MF} . (The form suggests equal coupling strength J'_{MF} to n ladders). In particular, the field dependencies of the ordering temperature T_c is given by Eq. (2) of Ref. [10]. In this formula the quantity A_x is the amplitude of AF correlations in isolated chains (Fig. 3(c)). Combined with the field dependence of $\langle S_z \rangle$, this gives us the field-temperature phase boundary shown in a solid line Fig. 4.

DIMPY was previously hailed as an almost perfect 1D system that even at $H > H_{c1}$ remains disordered [15]. In fact, more careful specific heat measurements reveal a weak but well defined lambda anomaly that appears for $H > H_{c1}$. This can be interpreted as the onset of 3D long-range order. Typical spin specific heat data collected in protonated samples for $H \parallel a$, are shown in Fig. 4 [33]. At each field, the putative ordering temperature T_c was identified with the peak position. It is plotted against field in symbols in Fig. 4 (right axis). The experimentally measured phase boundary is in excellent agreement with the chain-MF prediction assuming an unfrustrated inter-ladder coupling of $nJ'_{\text{MF}} = 6.3 \mu\text{eV}$. This agreement lends credence that the singularity seen in specific heat is indeed associated with the 3D ordering.

As MF neglects the quantum fluctuations between the ladders, J'_{MF} may underestimate the real coupling J' . This said, given almost the same inter-ladder MF coupling as in the strong-rung material BPCB ($nJ'_{\text{MF}} = 6.9 \mu\text{eV}$ [10]), the ordering temperature is considerably enhanced in the strong-leg case of DIMPY. This effect is principally due to the rapid growth of transverse correlations as defined by A_x , and their slow falloff due to the large K , showing again the differences between the strong leg and strong rung limits.

This work is partially supported by the Swiss National Fund under MaNEP and Division II. We thank T. Yankova for her involvement in the synthesis of DIMPY samples.

Note added: During the final stage of this work we became aware of the study by Ninios *et al.*, arXiv:1110.5653v1, which contains experimental data similar to those shown in Fig. 4.

* zhelud@ethz.ch; <http://www.neutron.ethz.ch/>

- [1] T. Giamarchi, C. Rugg, and O. Tchernyshev, *Nature Physics* **4**, 198 (2008).
 [2] E. Dagotto and T. M. Rice, *Science* **271**, 5249 (1996).
 [3] T. Giamarchi, *Quantum Physics in One Dimension*

(Clarendon Press, 2003).

- [4] T. Giamarchi and A. M. Tsvelik, *Phys. Rev. B* **59**, 11398 (1999).
 [5] T. Masuda *et al.*, *Phys. Rev. Lett.* **96**, 047210 (2006).
 [6] V. O. Garlea *et al.*, *Phys. Rev. Lett.* **98**, 167202 (2007).
 [7] A. Zheludev *et al.*, *Phys. Rev. B* **76**, 054450 (2007).
 [8] C. Lorenz *et al.*, *Phys. Rev. Lett.* **100**, 067208 (2008).
 [9] C. Rüegg *et al.*, *Phys. Rev. Lett.* **100**, 25701 (2008).
 [10] M. Klanjšek *et al.*, *Phys. Rev. Lett.* **101**, 137207 (2008).
 [11] B. Thielemann *et al.*, *Phys. Rev. B* **79**, 020408 (2009).
 [12] B. Thielemann *et al.*, *Phys. Rev. Lett.* **102**, 107204 (2009).
 [13] A. T. Savici *et al.*, *Phys. Rev. B* **80**, 094411 (2009).
 [14] F. D. M. Haldane, *Phys. Rev. Lett.* **50**, 1153 (1983).
 [15] T. Hong *et al.*, *Phys. Rev. Lett.* **105**, 137207 (2010).
 [16] D. Schmidiger *et al.*, *Phys. Rev. B* **84**, 144421 (2011).
 [17] M. Popovici, *Acta Cryst.* **A31**, 507 (1975).
 [18] A. Shapiro *et al.*, *J. Am. Chem Soc* **129**, 952 (2007).
 [19] A. Daley, C. Kollath, U. Schollwöck, and G. Vidal, *J. Stat. Mech.: Theor. Exp.* **2004**, P04005 (2004).
 [20] S. R. White, *Phys. Rev. Lett.* **69**, 2863 (1992).
 [21] P. Bouillot *et al.*, *Phys. Rev. B* **83**, 054407 (2011).
 [22] Supplementary material.
 [23] T. Barnes, E. Dagotto, J. Riera, and E. S. Swanson, *Phys. Rev. B* **47**, 3196 (1993).
 [24] S. Notbohm *et al.*, *Phys. Rev. Lett.* **98**, 027403 (2007).
 [25] O. P. Sushkov and V. N. Kotov, *Phys. Rev. Lett.* **81**, 1941 (1998).
 [26] C. Knetter, K. P. Schmidt, M. Grüninger, and G. S. Uhrig, *Phys. Rev. Lett.* **87**, 167204 (2001).
 [27] To subtract the background, we repeated the same scans at $T = 50$ K and $T = 100$ K, where the magnetic contribution is expected to be wiped out. The signal at high temperature was decomposed into T -dependent and T -independent parts, assuming that the latter is due to phonons and therefore scales with the Bose factor. From this analysis the combined background was calculated for $T = 1.5$ K and subtracted from the data shown. All operations were performed point-by-point.
 [28] D. A. Tennant *et al.*, *Phys. Rev. B* **67**, 054414 (2003).
 [29] T. Hikihara and A. Furusaki, *Phys. Rev. B* **63**, 134438 (2000).
 [30] The data were collected on a Quantum Design Magnetic Properties Measurements System MPMS-XL with an iQuantum ^3He refrigerator. $g = 2.17$ is known from the independently measured gap energy and critical field.
 [31] Note the factor 2 difference compared to Eq. (2) in Ref. [15]. In our notation, specific heat is calculated *per spin*, as is customary [3], and not per rung. Our measured C/T values are in good agreement with the experimental data in [15].
 [32] D. J. Scalapino, Y. Imry, and P. Pincus, *Phys. Rev. B* **11**, 2042 (1975).
 [33] The data were collected on a Quantum Design Physical Properties Measurement System with a ^3He - ^4He dilution refrigerator. The calculated Shottky contribution of nuclear spin was subtracted. In the studied temperature range lattice contribution to specific heat is totally negligible.